Immunologic Research (2019) 67:202–211
https://doi.org/10.1007/s12026-019-09084-w

ORIGINAL ARTICLE

B7-H3 modulates endothelial cell angiogenesis through the VEGF cytokine

Huijun Lai[1,2] · Zhongwen Sun[3] · Jie Yang[3] · Pingping Wu[3] · Yundi Guo[3] · Jing Sun[3]

Published online: 10 July 2019

Abstract

B7-H3 is a cell surface molecule in the immunoglobulin superfamily that has been shown to perform both immunological and non-immunological functions. It has also been found that vascular endothelial growth factor (VEGF) is an important molecule in the modulation of endothelial cell behavior. In this study, we analyzed the serum expression of B7-H3 in 113 rheumatoid arthritis and systemic lupus erythematous patients using the ELISA and found a positive correlation between B7-H3 and VEGF. Next, we investigated the involvement of B7-H3 in angiogenesis using human umbilical vein endothelial cells (HUVECs) with transient knockdown of B7-H3 and an in vivo Matrigel model. Data from the in vitro experiments showed that B7-H3 increased cell proliferation, migration, and tube formation, and correlated with the expression of VEGF. Furthermore, B7-H3 affected the formation of functional vascular networks in Matrigel plugs, which were dissected from mice injected with different HUVECs. Our data suggest that B7-H3 promotes angiogenesis through the enhancement of VEGF secretion. This is the first study proposing a significant role for B7-H3 in the promotion of angiogenesis and may provide further understanding of this gene's biological function.

Keywords B7-H3 · Costimulatory molecule · VEGF · Angiogenesis

Introduction

B7-H3, also known as CD276, is a member of the B7 costimulatory molecules and was first identified in 2000 [1]. T cells, natural killer (NK) cells, antigen-presenting cells (APCs), and some non-immune cells, such as osteoblasts [2, 3], fibroblasts, fibroblast-like synoviocytes [4], and epithelial cells [5], have been shown to express the B7-H3 protein. Numerous studies have demonstrated the involvement of B7-H3 in the regulation of immune responses, including T cell activation or inhibition [6, 7]. Interestingly, B7-H3 has also been found to play a role in tumor migration [8, 9], cell interaction [4], and osteoclast differentiation [2]. An increasing number of studies now indicate the importance of this B7 homolog molecule in non-immunological functions.

Angiogenesis, the formation of new blood vessels, is crucial in a number of physiological processes as well as inflammatory diseases, including rheumatoid arthritis (RA) and systemic lupus erythematosus (SLE) [10, 11]. RA angiogenesis is driven and maintained by proangiogenic factors, such as vascular endothelial growth factor (VEGF), angiopoietin (Ang) 1 and 2, platelet-derived growth factor, and transforming growth factor-β [12–14]. VEGF is highly expressed in RA, and is the most potent proangiogenic factor in RA angiogenesis [15].

Recently, B7-H3 has been implicated as a potential regulator of antitumor immunity [16–18]. We have previously reported the aberrant expression of B7-H3 in autoimmune diseases including RA, SLE, and scleroderma [19–21]. Moreover, B7-H3 expression correlates with clinical disease parameters [20]. Is B7-H3 involved in angiogenesis in the above diseases? Is there any correlation between B7-H3 and VEGF? The aim of this present study was to extend our previous findings and validate the crucial role of B7-H3 in angiogenesis.

Huijun Lai and Zhongwen Sun contributed equally to this work.

✉ Jing Sun
jsun@szhct.edu.cn

[1] Soochow University, Suzhou 215009, Jiangsu, People's Republic of China

[2] Ultrasound Institute, Suzhou Hospital of Traditional Chinese Medicine, Suzhou 215009, Jiangsu, People's Republic of China

[3] Institute of Medical Technology, Suzhou Vocational Health College, Suzhou 215009, Jiangsu, People's Republic of China

Materials and methods

Subjects

We obtained blood samples from RA ($n = 68$) and SLE ($n = 45$) patients from the Department of Rheumatology, Suzhou Hospital of Traditional Chinese Medicine, Jiangsu Province, China, from January 2013 through July 2015. Forty-three samples from healthy blood donors were collected in parallel as controls. Peripheral blood samples were centrifuged at 25 °C, 1000 rpm. Serum samples were stored at − 80 °C until further evaluation. All experiments were approved by the Ethics Review Board of Suzhou Vocational Health College, and written informed consent was obtained from each blood donor.

Primary human umbilical vein endothelial cells (HUVECs) were isolated from human umbilical cords that were obtained from the Second Affiliated Hospital of Nanjing Medical University. HUVECs were cultured in plates pre-coated with gelatin (Sigma-Aldrich, St. Louis, MO, USA) using Endothelial Cell Medium (ECM, ScienCell, Carlsbad, CA, USA) supplemented with 10% fetal bovine serum (FBS, GIBCO BRL, Grand Island, NY, USA). Cells were incubated at 37 °C at 5% CO_2.

Plasmid construction, lentivirus production, and cell infection

Two short hairpin RNA (shRNA) sequences for B7-H3 and a non-target control were synthesized by the GenePharma Company (Suzhou, China). The B7-H3 shRNA sequence for the first CD276-1041 site was 5′GTGCTGGA GAAAGATCAAA 3′, and for the second CD276-996 site was 5′GCTGTCTGTCTGTCTCATT3′. We then constructed packaging plasmids using the cloned oligonucleotides. The infectious lentivirus vectors were generated and collected at 48-h post-transduction by infecting 293 T cells using packaging plasmids and a shuttle vector, namely pGLV3-H1-GFP-Puro. The hole-by-dilution titer assay was used to determine the virus titer ($\sim 5.0 \times 10^7$ TU/mL). HUVECs were infected with 5 μl of lentivirus in 6-well plates containing 5 μg/mL polybrene (Sigma-Aldrich, St. Louis, MO, USA) for 72 h. The infected cells were washed in fresh complete medium and used in all other subsequent experiments.

Real-time PCR and flow cytometry

Total RNA was isolated from the shRNA-infected cells using the RNeasy Mini Kit (Qiagen, Germany). RNA purification was performed prior to synthesizing cDNA using the genomic DNA extraction kit (RNase-Free DNase Set for DNase digestion). cDNA synthesis was performed with the PrimeScript™ RT reagent kit (TaKaRa, Tokyo, Japan), and real-time PCR was analyzed on the Bio-RAD iCycler CFX96. GAPDH was used as an endogenous control and all values were expressed as fold difference relative to the expression of GAPDH. PCR primer pairs were as follows: the sense of B7-H3: 5′-GGC TGT CTG TCT GTC TCA TTG-3′; the antisense of B7-H3: 5′-TCC ATC ATC TTC TTT GCT GTC A-3′; the sense of GAPDH: 5′-ATC TGG CAC CAC ACC TTC TAC A-3′; the antisense of β-actin: 5′-GAT AGC ACA GCC TGG ATA GCA A-3′.

Flow cytometry was performed simultaneously to determine the B7-H3 knockdown in infected HUVECs. Cells were washed in a fluorescence-activated cell sorter (FACS) buffer (phosphate-buffered saline supplemented with 1% bovine serum albumin and 0.1% NaN_3), and incubated with 1 μl APC-conjugated B7-H3 antibody (Biolegend, San Diego, CA, USA) for 30 min at 4 °C. After washing with the FACS buffer, cells were fixed with 1% (weight/volume) paraformaldehyde for 30 min and then stored in the dark for flow cytometric analysis. Cytofluorometry was analyzed by an Accuri C6 (Becton Dickinson, San Jose, CA, USA).

Cell proliferation assay

Cell proliferation was determined using the Cell Counting Kit-8 (CCK-8, Dojindo, Japan). Briefly, HUVECs were incubated in 96-well plates for 24 h at a density of 5000 cells/100 μl. In the B7-H3-Ig fusion protein group, HUVECs were incubated with 20 μg/mL B7-H3-Ig (R&D, Minneapolis, MN, USA). CCK-8 solution was added to the wells after 24 h according to the manufacturer's instructions, and cell proliferation was detected at 650 nm using a spectrophotometer (Thermo Fisher Scientific, Waltham, MA, USA). The cell proliferation experiment was performed in triplicate wells and repeated 4 times. At the same time, we added the VEGF inhibitor apatinib (MedChem Express, Monmouth Junction, NJ, USA) to one group. Apatinib is a selective VEGFR2 inhibitor with an IC50 of 1 nM. Cell proliferation was also performed using the Real Time Cellular Analysis (xCELLigence RTCA, Thermo Fisher Scientific, Waltham, MA, USA). Cells were seeded in E-Plate 16 PET at 3000 cells/50 μl. B7-H3-Ig (12 μg/mL) was added to selected wells, followed by the addition of 1640 cell medium. The impedance value of each well was automatically monitored by the system for a total of 96 h and expressed as the Cell Index (CI) value.

Cell migration assay

The rate of cell migration was monitored in real time with the xCELLigence RTCA DP system using CIM plates. Approximately 4 h prior to conducting the experiment, HUVECs were serum starved. The upper chambers of

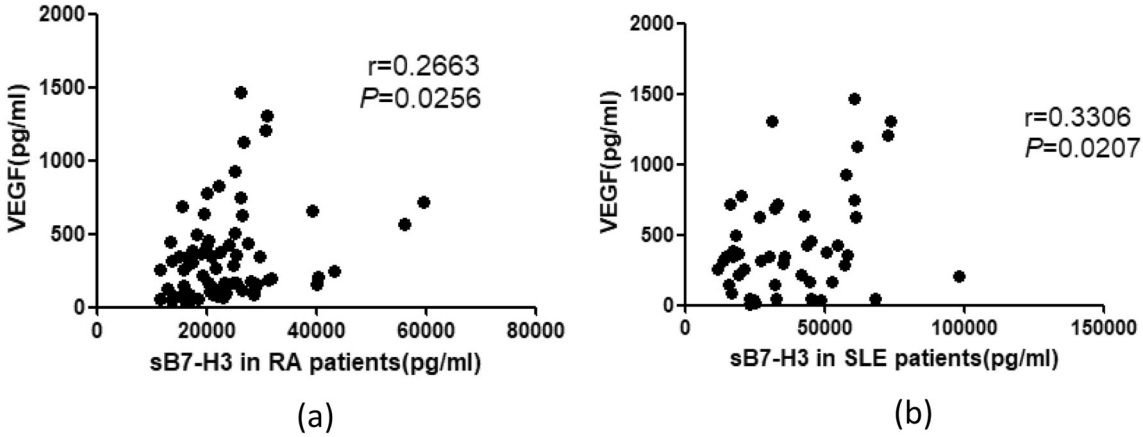

Fig. 1 Correlation between sB7-H3 and VEGF. Serum was obtained from the peripheral blood of rheumatoid arthritis (RA) and systemic lupus erythematosus (SLE) patients. Human VEGF and sB7-H3 protein levels were quantified using the ELISA. Nonlinear regression analysis was used to determine the correlation between the expression of B7-H3 and VEGF protein in **a** RA patients ($n = 68$) and **b** SLE patients ($n = 45$). $P < 0.05$ was considered statistically significant

the CIM plates were coated with 1 μg/mL of fibronectin. Cells in serum-free media were then added to the upper chambers (5000 cells per well) in the presence of either B7-H3-Ig or control His-tag protein at 12 μg/mL. HUVEC cultures were added to the lower chambers of each well. The CIM plates were left in an incubator for 1 h to allow cell attachment. The impedance value of each well was automatically monitored by the system for a total of 24 h and expressed as the CI value.

VEGF quantification

The HUVEC culture medium from the cell proliferation assays was collected and stored at − 80 °C until further analysis. A human VEGF ELISA kit was obtained from Abcam (Cambridge, MA, USA). VEGF protein levels were measured in the serum of RA and SLE patients, as well as the HUVEC culture medium (100 μl). The ELISA was performed according to the manufacturer's instructions. Protein levels were

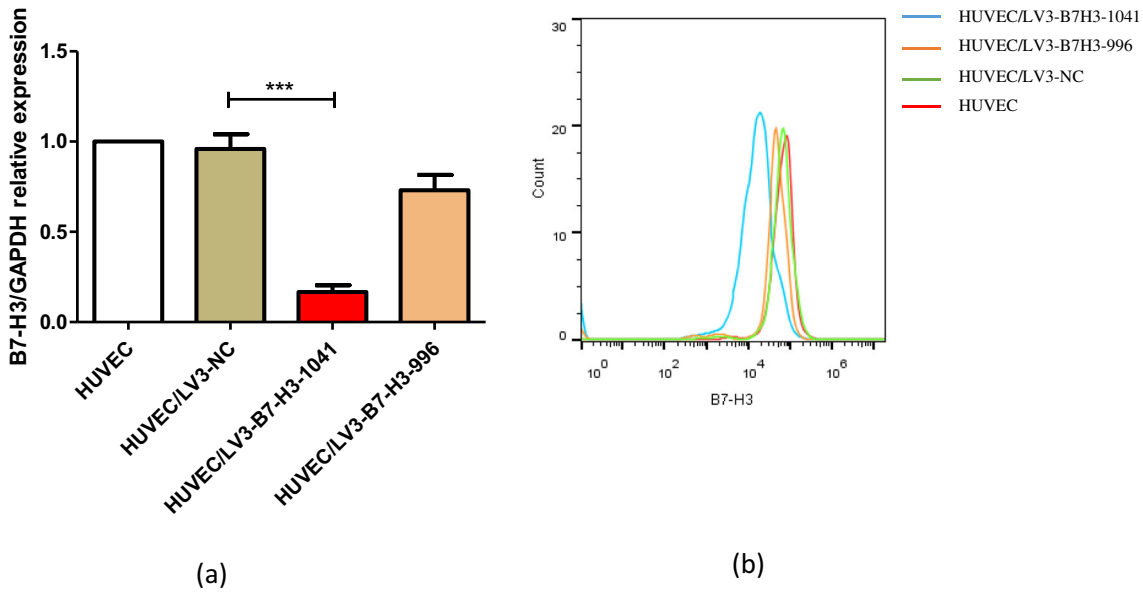

Fig. 2 Knockdown efficiency of B7-H3 shRNA in HUVECs. HUVECs were infected with shRNA from either B7-H3 or a non-target control gene. The levels of **a** B7-H3 mRNA and **b** B7-H3 protein in the infected cells were measured using Real-time PCR and flow cytometry, respectively. HUVEC/LV3-B7-H3-1041 and HUVEC/LV3-B7-H3-996 correspond to HUVECs transfected with virus-expressing B7-H3 shRNA. LV3-NC corresponds to the negative control of the non-target control gene

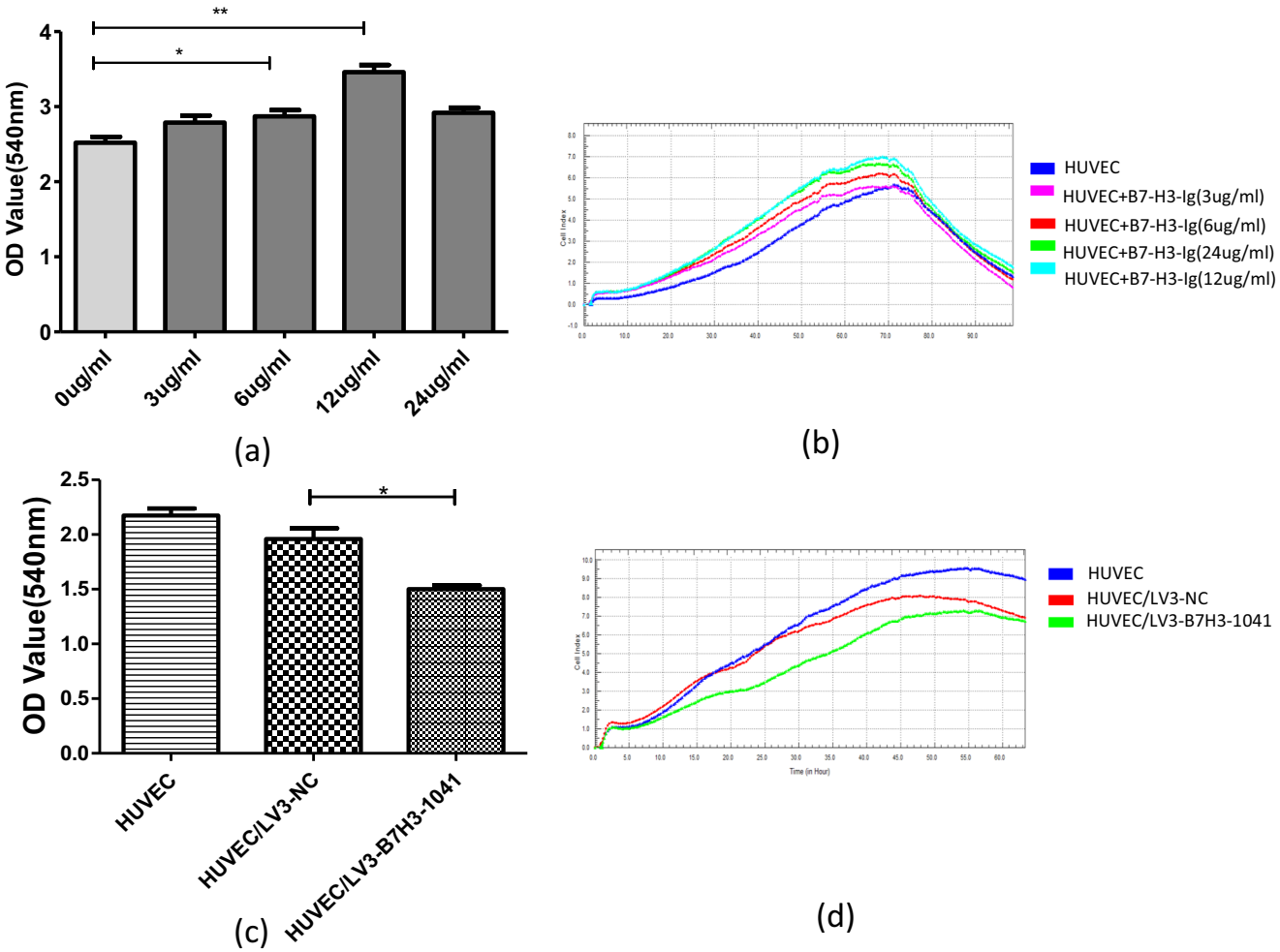

Fig. 3 Effect of B7-H3 on endothelial cell proliferation. **a** CCK-8 analysis and **b** the RTCA assay were performed on HUVECs incubated with 0–24 μg/mL B7-H3-Ig. Cell proliferation was analyzed in HUVECs with B7-H3 knockdown using **c** the CCK-8 assay and **d** the RTCA assay. The impedance value of each well was automatically monitored by the RTCA assay and was expressed as a Cell Index (CI) value. LV3-NC corresponds to the negative control. $*P < 0.01$; $**P < 0.05$

detected at 450 nm and quantified using an ELISA reader equipped with specialized software (Thermo Fisher Scientific, Waltham, MA, USA).

Angiogenesis assay

In the tube formation assay, HUVECs were seeded onto 15-well U-slide plates (1×10^4/well) pre-coated with 10 μl of growth factor–reduced Matrigel (BD Biosciences, Franklin Lakes, NJ, USA) in the presence of either B7-H3-Ig (12 μg/mL) or a control medium. After 6 h, calcein (Sigma-Aldrich, St. Louis, MO, USA) was added and the morphology of the capillary-like structures formed by the HUVECs was observed under an inverted microscope. Images were captured in 4 random microscopic fields with a computer-assisted microscope (Leica Factory, Germany). Tube length was quantified by measuring the cumulative tube length using the WimTube quantitative tube formation image analysis.

Matrigel plug assay

All animal experiments were approved by the Animal Experimentation Ethics Committee of the Suzhou Vocational Health College. C57BL/6 mice aged 6–8 weeks were obtained from the Animal Experiment Center of the Chinese Academy of Sciences (Shanghai, China). Control HUVECs or HUVECs with transient B7-H3 knockdown in combination with 500 μl Matrigel and 25 ng/mL VEGF were injected subcutaneously into the abdomens of C57BL/6 mice. Six mice were included in each treatment group. Mice were euthanized after an 8-day incubation period. Matrigel plugs were carefully removed by dissection. Surrounding connective tissue was excised and the plugs were fixed in 4% formalin, embedded in paraffin, and stained with hematoxylin and eosin, and the microvessel marker of CD105 monoclonal antibody (Boster, clone BA1725). Immunohistochemical staining for CD105 was performed according to the manufacturer's instructions. In brief, sections were cooled and immersed in 3% H2O2 solution for

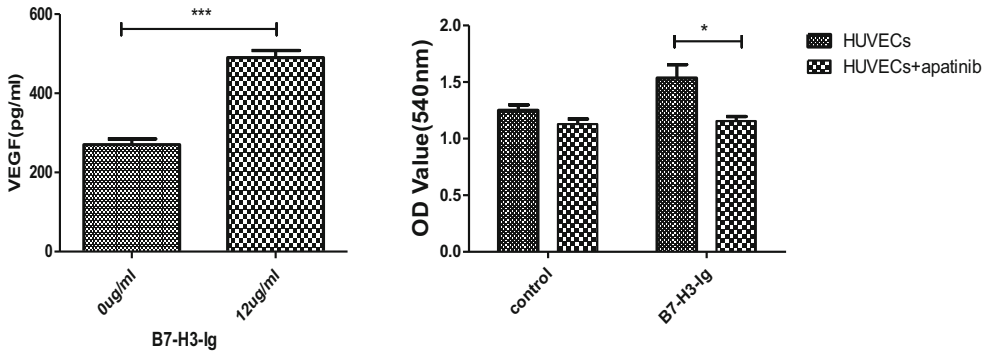

(a) (b)

Fig. 4 Effect of B7-H3 on HUVECs was partly related to VEGF. **a** Effect of B7-H3 on VEGF secretion from endothelial cells. HUVECs were incubated with 12 μg/mL B7-H3-Ig for 10 h. VEGF protein levels were quantified in the cell culture supernatant using an ELISA. **b** Apatinib (VEGF inhibitor) eliminated the effect of B7-H3. HUVECs were incubated with 1 μM apatinib and 12 μg/mL B7-H3-Ig. A CCK-8 assay was performed to count the number of cells

20 min to block the endogenous peroxidase activity, then rinsed in PBS for 5 min, blocked with 5% BSA at room temperature for 20 min, and incubated with primary antibodies against CD105 (1:50 dilution, 4 μg/mL final concentration) at 4 °C overnight. A universal biotinylated secondary antibody was then developed. Images were photographed using an Olympus BX43 microscope equipped with a digital camera (Olympus, Tokyo, Japan).

Statistical analysis

The statistical analysis was performed using GraphPad Prism 5 software (GraphPad software, Inc., La Jolla, CA, USA). The *t* test was used to analyze the data when a normal distribution was confirmed; otherwise, the nonparametric Mann-Whitney test was utilized. Nonlinear regression analysis was used to determine the correlation between the clinical examination indexes and the degree of disease activity as well as the correlation between the expression of sB7-H3 and VEGF. The correlations were determined based on the r^2 values. $P < 0.05$ was considered statistically significant.

Results

Soluble B7-H3 expression in the serum of RA and SLE patients correlates with VEGF expression

We analyzed soluble B7-H3 (sB7-H3) and VEGF expression in the serum of RA ($n = 68$) and SLE ($n = 45$) patients as well as healthy controls ($n = 56$) using the ELISA. Nonlinear regression analysis showed a positive correlation between the expression of sB7-H3 and VEGF levels in both RA (Fig. 1a) and SLE (Fig. 1b) patients, as well as in control subjects.

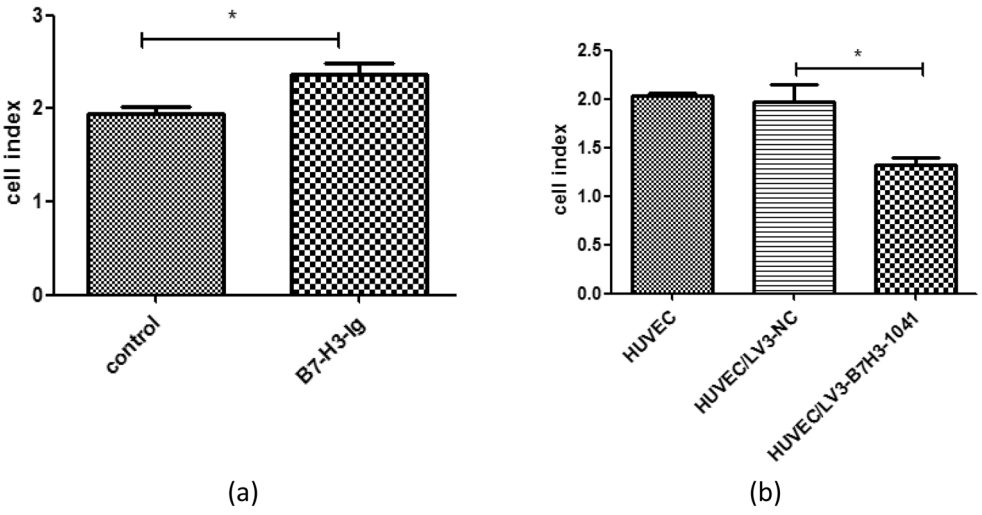

(a) (b)

Fig. 5 Effect of B7-H3 on the migration of endothelial cells. Cell migration was analyzed using the RTCA assay in **a** HUVECs incubated with 12 μg/mL B7-H3-Ig for 10 h and **b** HUVECs infected with LV3-B7-H3-1041 or LV3-NC for 10 h. The Cell Index reflects the number of cells migrating to the lower chamber from the upper chamber of the culture plate. $^*P < 0.05$

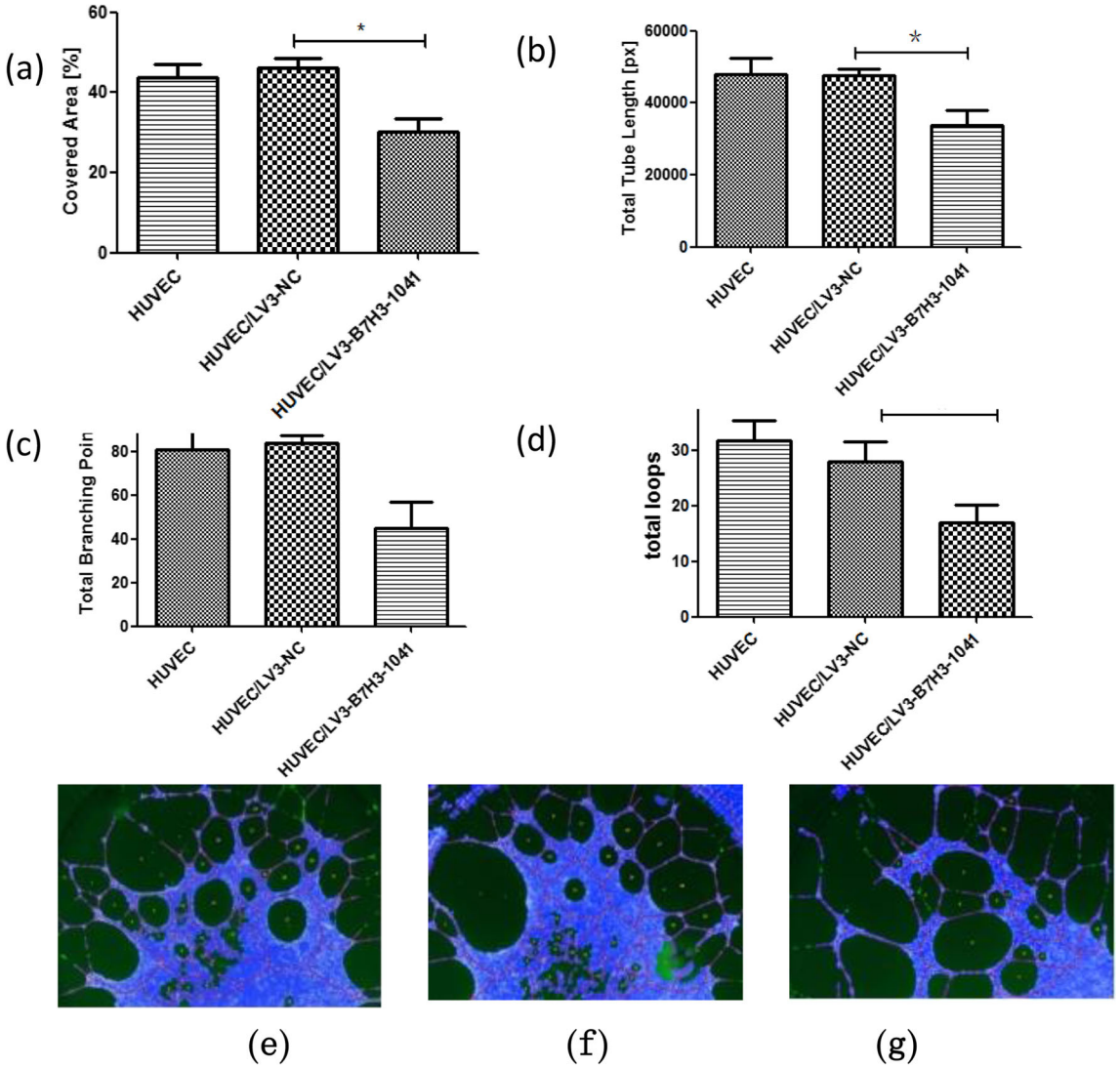

Fig. 6 Effect of B7-H3 on endothelial cell tube formation. HUVECs were seeded onto 15-well U-slide plates (1×10^4/well) pre-coated with 10 μl of growth factor–reduced Matrigel (BD Biosciences, Franklin Lakes, NJ, USA) in HUVEC/LV3-B7-H3-1041 or HUVEC/LV3-NC. The morphology of the capillary-like structures formed by HUVECs was observed under an inverted microscope using WimTube quantitative tube formation image analysis software. The experiments were repeated 3 times. **a** Covered area, **b** total tube length, **c** total branching points, and **d** total loops; Representative images of tube formation in **e** HUVECs and **f** HUVECs infected with LV3-NC, and **g** HUVECs infected with LV3-B7-H3-1041

B7-H3-1041 shRNA efficiently reduces the expression of B7-H3 in human endothelial cells

The efficiency of B7-H3 shRNA virus infection in HUVECs was evaluated using real-time PCR and the flow cytometric assay (Fig. 2). HUVECs were infected with 2 different B7-H3 shRNAs corresponding to sites 1041 and 996 or with control shRNA. Real-time PCR showed that B7-H3 mRNA levels decreased efficiently when cells were infected with the shRNA-1041-site virus (LV3-B7H3-1041) compared with the non-targeting shRNA-infected (LV3-NC) control cells (Fig. 2a). From the real-time PCR data, we concluded that, compared with control cells, the mRNA levels of B7-H3 in HUVECs infected with LV3-B7H3-996 or LV3-B7H3-1041 were ~24% or ~84.7% lower, respectively. Flow cytometric analysis was performed to confirm these findings. As expected, we found decreased expression of B7-H3 in HUVECs infected with LV3-B7H3-1041 (Fig. 2b). Based on these data, we performed B7-H3 knockdown in HUVECs using LV3-B7H3-1041 in all subsequent experiments.

B7-H3 promotes the proliferation of human endothelial cells and VEGF secretion

CCK-8 and RTCA assays were performed to test the effect of B7-H3 on endothelial cell proliferation. HUVECs were either incubated with B7-H3-Ig or infected with LV3-B7H3-1041. As shown in Fig. 3a, B7-H3-Ig increased the proliferation of

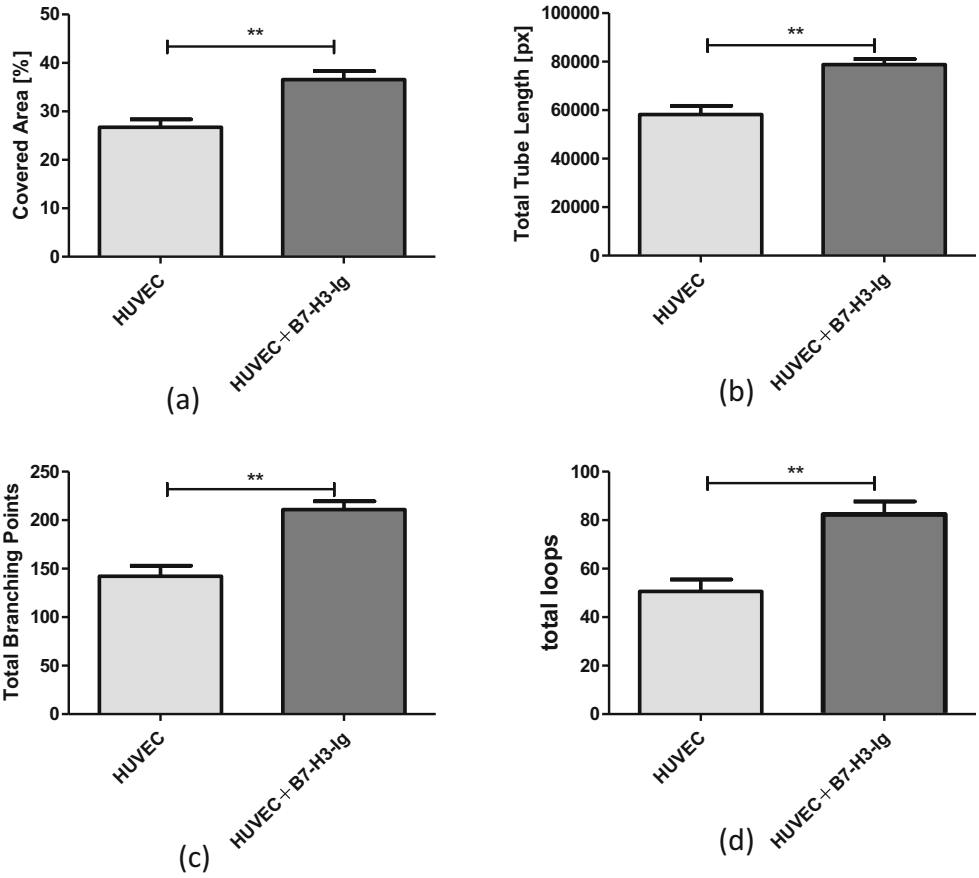

Fig. 7 Effects of B7-H3-Ig on endothelial cell tube formation. HUVECs were seeded onto 15-well U-slide plates (1×10^4/well) pre-coated with 10 μl growth factor–reduced Matrigel (BD Biosciences, Franklin Lakes, NJ, USA) in the presence of B7-H3-Ig (12 μg/mL) or a control medium. The morphology of capillary-like structures formed by HUVECs was observed under an inverted microscope using Image J software. **a** Covered area, **b** total tube length, **c** total branching points, and **d** total loops

HUVECs in a dose-dependent manner (the OD value increased 10.6% at 3 μg/mL, 13.9% at 6 μg/mL, 37.6% at 12 μg/mL, and 19.2% at 24 μg/mL). RTCA analysis also showed a dose-dependent increase in cell proliferation after incubation with B7-H3-Ig (Fig. 3b). B7-H3 knockdown with shRNA significantly inhibited cell growth after 24 h ($P = 0.0118$), whereas infection with LV3-NC had no effect on cell proliferation (Fig. 3c). Using the RTCA assay, we observed that the inhibition effect mainly occurred between 10 and 55 h after infection (Fig. 3d). Further, we analyzed the VEGF concentration in HUVECs with B7-H3-Ig and found that VEGF was significantly higher in the presence of B7-H3 (Fig. 4a). Given this, we added a group with the VEGF inhibitor apatinib to the proliferation assays. Apatinib significantly inhibited cell proliferation at 1 μM after incubating with HUVECs for 48 h. At the same time, we found apatinib eliminated the effect of adding B7-H3-Ig to HUVECs ($P < 0.05$, Fig. 4b).

B7-H3 promotes the migration of human endothelial cells

Subsequently, we evaluated the effects of B7-H3-Ig on HUVEC adhesion in vitro using the RTCA assay. After 3 h, HUVECs incubated with the B7-H3-Ig exhibited a much stronger adhesion to fibronectin (FN)-coated plates compared with negative control. Cell migration with B7-H3-Ig increased by ~ 21.5% compared with controls at 10 h ($P < 0.05$; Fig. 5a). Moreover, knockdown of B7-H3 transcripts using LV3-B7H3-1041 infection significantly delayed cell migration. Cell migration with B7-H3 knockdown decreased ~ 31.6% compared with the non-targeting shRNA control cells (Fig. 5b).

B7-H3 promotes endothelial cell tube formation in human endothelial cells

The tube formation assay is one of the simplest and most well-established in vitro angiogenesis assays. It is based on the ability of endothelial cells to form three-dimensional capillary-like tubular structures when cultured on a gel of growth factor–reduced basement membrane extracts. To evaluate the role of B7-H3 in this process, HUVECs treated with either LV3-NC or LV3-B7H3-1041 were plated on a thin layer of Matrigel and fixed after 24 h. Tube parameters (covered area, tube lengths, branching points, and loops) were calculated using Tube Formation Image Analysis 30001 software-WimTube (ibidi, Martinsried, German). As shown in Fig. 6a–d, the covered area, tube lengths, branching points, and loops formed by the B7-H3 knockdown cells were all ~ 40% diminished compared with the control cells, suggesting that B7-H3 possesses tubulogenic properties. Figure 6e–g show a representative image of the

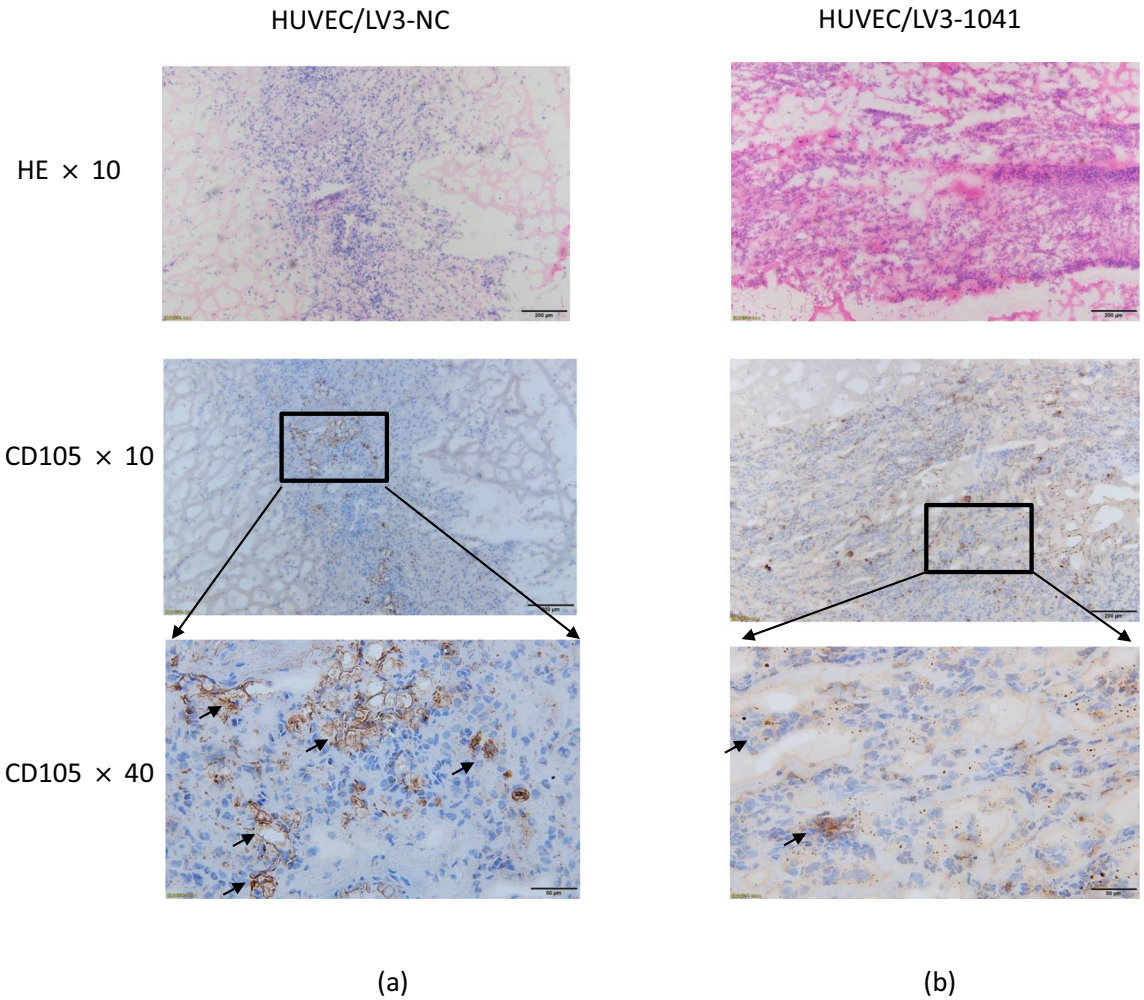

Fig. 8 Effect of B7-H3 on in vivo Matrigel plugs. Control HUVECs or HUVECs with transient B7-H3 knockdown in combination with Matrigel and VEGF were injected subcutaneously into C57BL/6 mice. The mice were euthanized after 8 days, and the Matrigel plugs were dissected and stained with hematoxylin and eosin, and anti-CD105. Images were photographed using an Olympus BX43 microscope equipped with a digital camera (Olympus, Tokyo, Japan). Representative images of HUVECs infected with **a** HUVEC/LV3-NC ($n = 6$) and **b** HUVEC/LV3-B7-H3-1041 ($n = 6$). Arrows indicate the locations of angiogenesis in the mouse Matrigel plug

predominant tube formation. Furthermore, we evaluated the effects of the B7-H3 fusion protein on HUVEC tube formation and found that B7-H3-promoted HUVECs also possess tubulogenic properties (Fig. 7).

Finally, we examined the function of B7-H3 in angiogenesis using the in vivo Matrigel model. In this assay, HUVECs with VEGF compounds were loaded into liquid Matrigel, which solidifies after subcutaneous injection and permits penetration by host cells as well as the formation of new blood vessels. After 8 days, the Matrigel plug was dissected, fixed, and stained with hematoxylin and eosin. Images of it were photographed and assessed for angiogenesis. As shown in Fig. 8, B7-H3 knockdown decreased the tube formation ability of HUVECs. These results are consistent with our in vitro assay findings. The anti-CD105 antibody microvessel-stained gel plugs were analyzed; representative results are shown in Fig. 8. In Fig. 8a, the upper panels are HE staining and the lower panels are CD105 staining. The number of microvessels of B7-H3 knockdown groups (HUVEC/LV3-1041) was substantially reduced compared with the NC controls. Images of the microvessels were assessed for angiogenesis.

Discussion

We report for the first time a new function of the B7-H3 protein: modulating endothelial cell angiogenesis. B7-H3 is a transmembrane glycoprotein, previously known as an immunoregulatory molecule, and expressed in T cells, natural killer (NK) cells, and antigen-presenting cells APCs. A number of studies, however, have shown that B7-H3 expression is not limited to immune cells. Osteoblasts [3, 22], fibroblasts [4], fibroblast-like synoviocytes, and epithelial cells [23] have also been shown to express the B7-H3 protein. This broad

expression pattern suggests that B7-H3 may have more diverse immunological, and most likely non-immunological, functions [24, 25].

In previous research, we analyzed the B7-H3 expression in autoimmune diseases, including RA and SLE [19, 20]. In this study, we found a significant correlation between the levels of soluble B7-H3 and VEGF in the serum of patients with RA and SLE. Moreover, numerous studies have reported that CD276/B7-H3 protein is expressed not only in angiogenic tumor vasculature, but also in established vasculature that has been co-opted by the tumor [26, 27]. We therefore hypothesized that B7-H3 may be involved in endothelial cell angiogenesis. To test this hypothesis, we constructed an endothelial cell line with B7-H3 knockdown and performed in vitro and in vivo assays using these cells.

The in vitro angiogenesis assay [28] confirmed our hypothesis that decreasing or inhibiting the levels of B7-H3 protein results in reduced cell proliferation, migration, and endothelial cell tube formation. Similarly, increased expression of B7-H3-Ig increases endothelial cell proliferation, migration, and tube formation. These data strongly suggest that B7-H3 plays a positive role in HUVEC angiogenesis. To further evaluate the mechanism of B7-H3 in HUVEC angiogenesis, we quantified the expression of VEGF that is secreted by HUVECs during endothelial cell tube formation. We found an increased expression of VEGF and a strong correlation with B7-H3 expression, implying that VEGF may participate along with B7-H3 to modulate endothelial cell angiogenesis. However, further exploration of this mechanism will have to wait until the B7-H3 receptor is discovered. It is therefore of crucial importance to identify the B7-H3 receptor in order to fully determine the diverse functions of B7-H3.

In summary, the data presented here provide evidence that B7-H3, a costimulatory molecule, may be involved in angiogenesis in autoimmune diseases such as RA and SLE. Our results show that B7-H3 plays an important role in endothelial cell proliferation, migration, and tube formation. More research is needed to fully investigate the potential role of B7-H3 as an angiogenic factor in other vascular-related disorders.

Funding This work was supported by grants from the Jiangsu Province University Outstanding Science and Technology Innovation Team (Grant no. 2015023), Qinglan Project (Sunjing, Sunzhongwen), and Jiangsu Provincial Medical Talent (Sunjing). The funders had no role in the study design, data collection and analysis, decision to publish, or preparation of the manuscript.

Compliance with ethical standards

All experiments were approved by the Ethics Review Board of Suzhou Vocational Health College, and written informed consent was obtained from each blood donor.

Conflict of interest The authors declare that they have no conflicts of interest.

References

1. Chapoval AI, Ni J, Lau JS, Wilcox RA, Flies DB, Liu D, et al. B7-H3: a costimulatory molecule for T cell activation and IFN-gamma production. Nat Immunol. 2001;2(3):269–74.
2. Suh WK, Wang SX, Jheon AH, Moreno L, Yoshinaga SK, Ganss B, et al. The immune regulatory protein B7-H3 promotes osteoblast differentiation and bone mineralization. Proc Natl Acad Sci U S A. 2004;101(35):12969–73.
3. Xu L, Zhang G, Zhou Y, Chen Y, Xu W, Wu S, et al. Stimulation of B7-H3 (CD276) directs the differentiation of human marrow stromal cells to osteoblasts. Immunobiology. 2011;216(12):1311–7.
4. Tran CN, Thacker SG, Louie DM, Oliver J, White PT, Endres JL, et al. Interactions of T cells with fibroblast-like synoviocytes: role of the B7 family costimulatory ligand B7-H3. J Immunol. 2008;180(5):2989–98.
5. Calabro L, Sigalotti L, Fonsatti E, Bertocci E, Di Giacomo AM, Danielli R, et al. Expression and regulation of B7-H3 immunoregulatory receptor, in human mesothelial and mesothelioma cells: immunotherapeutic implications. J Cell Physiol. 2011;226(10):2595–600.
6. Lee YH, Martin-Orozco N, Zheng P, Li J, Zhang P, Tan H, et al. Inhibition of the B7-H3 immune checkpoint limits tumor growth by enhancing cytotoxic lymphocyte function. Cell Res. 2017;27(8):1034–45.
7. Luo L, Chapoval AI, Flies DB, Zhu G, Hirano F, Wang S, et al. B7-H3 enhances tumor immunity in vivo by costimulating rapid clonal expansion of antigen-specific CD8+ cytolytic T cells. J Immunol. 2004;173(9):5445–50.
8. Li Y, Yang X, Wu Y, Zhao K, Ye Z, Zhu J, et al. B7-H3 promotes gastric cancer cell migration and invasion. Oncotarget. 2017;8(42):71725–35.
9. Li Y, Guo G, Song J, Cai Z, Yang J, Chen Z, et al. B7-H3 promotes the migration and invasion of human bladder cancer cells via the PI3K/Akt/STAT3 signaling pathway. J Cancer. 2017;8(5):816–24.
10. Marrelli A, Cipriani P, Liakouli V, Carubbi F, Perricone C, Perricone R, et al. Angiogenesis in rheumatoid arthritis: a disease specific process or a common response to chronic inflammation? Autoimmun Rev. 2011;10(10):595–8.
11. Leblond A, Allanore Y, Avouac J. Targeting synovial neoangiogenesis in rheumatoid arthritis. Autoimmun Rev. 2017;16(6):594–601.
12. Nagashima M, Yoshino S, Ishiwata T, Asano G. Role of vascular endothelial growth factor in angiogenesis of rheumatoid arthritis. J Rheumatol. 1995;22(9):1624–30.
13. Zhang J, Li C, Zheng Y, Lin Z, Zhang Y, Zhang Z. Inhibition of angiogenesis by arsenic trioxide via TSP-1-TGF-beta1-CTGF-VEGF functional module in rheumatoid arthritis. Oncotarget. 2017;8(43):73529–46.
14. Jiang S, Li Y, Lin T, Yuan L, Wu S, Xia L, et al. IL-35 inhibits angiogenesis through VEGF/Ang2/Tie2 pathway in rheumatoid arthritis. Cell Physiol Biochem. 2016;40(5):1105–16.
15. Clavel G, Bessis N, Boissier MC. Recent data on the role for angiogenesis in rheumatoid arthritis. Joint Bone Spine. 2003;70(5):321–6.
16. Efremova M, Rieder D, Klepsch V, Charoentong P, Finotello F, Hackl H, et al. Targeting immune checkpoints potentiates immunoediting and changes the dynamics of tumor evolution. Nat Commun. 2018;9(1):32.
17. Karin N. Chemokines and cancer: new immune checkpoints for cancer therapy. Curr Opin Immunol. 2018;51:140–5.
18. Hofmeyer KA, Ray A, Zang X. The contrasting role of B7-H3. Proc Natl Acad Sci U S A. 2008;105(30):10277–8.

19. Sun J, Lai H, Shen D, Wu P, Yang J, Sun Z, et al. Reduced sB7-H3 expression in the peripheral blood of systemic lupus erythematosus patients. J Immunol Res. 2017;2017:5728512.
20. Sun J, Liu C, Gao L, Guo Y, Zhang Y, Wu P, et al. Correlation between B7-H3 expression and rheumatoid arthritis: a new polymorphism haplotype is associated with increased disease risk. Clin Immunol. 2015;159(1):23–32.
21. Jiang J, Liu C, Zhang G, Gao L, Chen Y, Zhu R, et al. Enhancement of membrane B7-H3 costimulatory molecule but reduction of its soluble form in multiple sclerosis. J Clin Immunol. 2013;33(1):118–26.
22. Zhao JL, Chen FL, Zhou Q, Pan W, Wang XH, Xu J, et al. B7-H3 protein expression in a murine model of osteosarcoma. Oncol Lett. 2016;12(1):383–6.
23. Yan R, Yang S, Sun J, Chen X, Zhang G, Feng P, et al. A novel monoclonal antibody against mouse B7-H3 developed in rats. Hybridoma (Larchmt). 2012;31(4):267–71.
24. Feng P, Zhang H, Zhang Z, Dai X, Mao T, Fan Y, et al. The interaction of MMP-2/B7-H3 in human osteoporosis. Clin Immunol. 2016;162:118–24.
25. Li D, Wang J, Zhou J, Zhan S, Huang Y, Wang F, et al. B7-H3 combats apoptosis induced by chemotherapy by delivering signals to pancreatic cancer cells. Oncotarget. 2017;8(43):74856–68.
26. Seaman S, Zhu Z, Saha S, Zhang XM, Yang MY, Hilton MB, et al. Eradication of tumors through simultaneous ablation of CD276/B7-H3-positive tumor cells and tumor vasculature. Cancer Cell. 2017;31(4):501–15.
27. Qin X, Zhang H, Ye D, Dai B, Zhu Y, Shi G. B7-H3 is a new cancer-specific endothelial marker in clear cell renal cell carcinoma. Onco Targets Ther. 2013;6:1667–73.
28. Nowak-Sliwinska P, Alitalo K, Allen E, Anisimov A, Aplin AC, Auerbach R, et al. Consensus guidelines for the use and interpretation of angiogenesis assays. Angiogenesis. 2018;21(3):425–532.